Renewable Energy 223 (2024) 120044

Contents lists available at ScienceDirect

Renewable Energy

journal homepage: www.elsevier.com/locate/renene

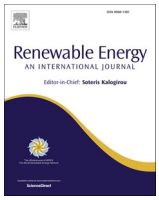

Synchronized optimization of wind farm start-stop and yaw control based on 3D wake model

Quan Wang [a,b,*], Tangjie Xu [a], Dominic von Terzi [b], Wei Xia [a], Zhenhai Wang [a], Haoran Zhang [a]

[a] College of Mechanical Engineering, Hubei University of Technology, Wuhan, China
[b] Faculty of Aerospace Engineering, Delft University of Technology, Delft, Netherlands

ARTICLE INFO

Keywords:
Wind farm layout
Start-stop
yaw control
3D wake model
Optimization

ABSTRACT

In existing wind farms, the overall power output can be increased through yaw control. However, the cooperative control of start/stop, yaw and turbines positions is often overlooked, leading to wake superposition to downstream wind turbines and suboptimal power output. This paper proposes a synchronized optimized method that considers start/stop, yaw and turbines positions control based on a three-dimensional wake model and yaw flow superposition model. The objective function of the proposed strategy is to maximize the power output of the Chapman Ranch (CR) wind farm. Four cases are considered: start-stop, yaw control, start-stop & yaw control and start-stop & yaw & turbines positions control. The particle swarm algorithm is introduced to optimize the wind farm layout. According to the results, considering start-stop, yaw and turbines positions optimization can not only increase the annual power output of the wind farm by 8.85 %, but also avoid the colliding wake in the CR wind farm. However, the other three cases will cause colliding wake in some fields of the CR wind farm. This study provides important guidance on improving the overall power output of existing wind farms.

1. Introduction

Wind energy is a renewable source of energy. Optimizing the layout of wind farms can enhance energy output and reduce energy costs. However, most researchers primarily concentrate on wind farm layout optimization using various algorithms, while paying little attention to the start/stop and yaw control aspects in real wind farms. This paper aims to investigate wind farm layout optimization by considering integrated start/stop and yaw control.

1.1. Wake model study

Modern wind farms often consist of a dense arrangement of wind turbines within a confined area. Minimizing wake interference between turbines is crucial to enhance the overall power output of the wind farm. During the design and optimization of wind farm layouts, wake models are commonly utilized to calculate the wake velocity between individual turbines. The Jensen wake model [1] is a widely employed semi-empirical wake model. Subsequently, Kayic [2] and Frandsen [3] made improvements to the Jensen model, although deviations from experimental data persisted [4,5].To address these limitations, Takeshi [6] proposed a novel wake model that accounts for ambient turbulence intensity and the effects of the thrust coefficient. The study demonstrated good agreement between the predicted velocity deficit, added turbulence intensity, and the results obtained from large eddy simulations (LES) and experimental data. Majid Bastankah [7] introduced a three-dimensional wake model based on the principles of mass and momentum conservation. The model requires obtaining the wake expansion factor through fluid mechanics analysis. Another contribution by Siyu Tao [8] involved the development of a newly devised 3D Gaussian wake model, which was successfully applied to wind farm layout optimization. The results indicated the model's effectiveness in addressing the optimization problem of wind farm layouts. Guo-Wei Qian [9] introduced a novel multiple wake model that took into account local effective turbulence and wake interaction effects. His research suggested a yaw offset limit of $\pm 15^{\circ}$to ensure the maximization of power production. Rezvane S [10] presented an innovative method to compute the turbine's inflow speed by considering wake interactions in a wind farm. using this method, the power output of a hypothetical wind farm was calculated. The efforts of these researchers have greatly enriched the body of knowledge on wake models, providing valuable tools for calculating inflow wind speed and turbulence intensity in wind

* Corresponding author. Hubei University of Technology Delft University of Technology, Netherlands.
E-mail address: quan_wang2003@163.com (Q. Wang).

https://doi.org/10.1016/j.renene.2024.120044
Received 14 August 2023; Received in revised form 26 December 2023; Accepted 21 January 2024
Available online 23 January 2024

farms.

1.2. Wind farm layout optimization

The wake effect caused by upstream wind turbines significantly impacts the power generation of downstream wind turbines. As the number of turbines in a wind farm increases, the disturbance caused by the wake effect becomes more pronounced, leading to reduced power generation efficiency. Howland [11] reported that wake offset could reach up to 0.6D. Fleming [12] conducted field experiments that verified the effectiveness of yaw control in enhancing wind farm power generation. Gebraad [13] utilized computational fluid dynamics (CFD) simulations to investigate the performance of three-row and two-row wind farms comprising six turbines, observing that yaw angle control can increase the power output of wind farms. Hongliang Ma [14] studied cooperative yaw control for aligned turbines to maximize power production, and the results demonstrated its effectiveness. Park [15] proposed a data-driven method based on a Bayesian ascent algorithm to optimize total wind farm power by dynamically controlling pitch and yaw angles of turbines. Bingzheng [16] described a yaw angle optimization strategy that maximized power output, leading to improvements of up to 7 % in an offshore wind farm. Haces [17] introduced a concept for modifying wind farm layout by deactivating specific turbines to maximize total power output. Zhenyu Lei [18] proposed a genetic learning particle swarm optimization approach with an adaptive strategy (AGPSO) for wind farm layout optimization, achieving high conversion efficiencies under various wind scenarios. Qingshan Yang [19] presented a hybrid optimization strategy that combined an analytical wake model with wind farm layout optimization, leading to a 1.9 % decrease in the cost of energy. Shriya V [20]. proposed a local, continuous refinement method to optimize wind farm layout. According to the results, this method surpassed the compared refinement technique by producing layouts that enhance overall energy production, leading to a reduction in the LCOE. Lichao Cao [21] introduced a multi-objective framework considering both power generation and turbulence intensity distribution in wind farms, resulting in a layout with increased total power (0.8 % improvement) and reduced turbulence intensity (8.1 % reduction). Yi Wen [22] employed a risk management method, based on conditional value-at-risk, to optimize the wind farm layout with uncertain wind condition. The results showed that this method could constrain the error in AEP and power fluctuations more effectively than traditional optimized method. Furthermore, some other researchers [23–26] have also have made significant contributions to the field of wind farm layout optimization, introducing diverse ideas and strategies to maximize overall energy production.

1.3. The main work in this paper

The aforementioned studies have significantly advanced the fields of wake modeling, wind farm layout optimization, and yaw control. While some have honed in on improving the precision of wake models for velocity prediction, others have delved into wind farm layout optimization using various intelligent algorithms. A third group has explored optimizing the yaw angle of wind turbines within specific wind farms. However, for existing wind farms, altering turbines locations is challenging. The feasible approach is to control the start-stop mechanism and yaw angle of the turbines to enhance overall power production. Yet, few researchers have concentrated on the synchronizing start/stop, yaw angle control and turbines positions to boost overall power output.

The structure of this paper is illustrated in Fig. 1. Initially, the wake velocity and wind turbine power are calculated based on the 3D-wake offset model and the prevailing wind resource conditions, as discussed in Sections 2 and 3. Subsequently, an optimization mathematical model is constructed for a wind farm, taking into account four different cases: yaw control (case 1), start-stop (case 2), start-stop & yaw control (case 3) and start-stop, yaw control and turbines positions (case 4). In section 4, we delve into the optimization results for four scenarios, examining both specific and annual wind conditions. The paper concludes with key findings and implications summarized in Section 5.

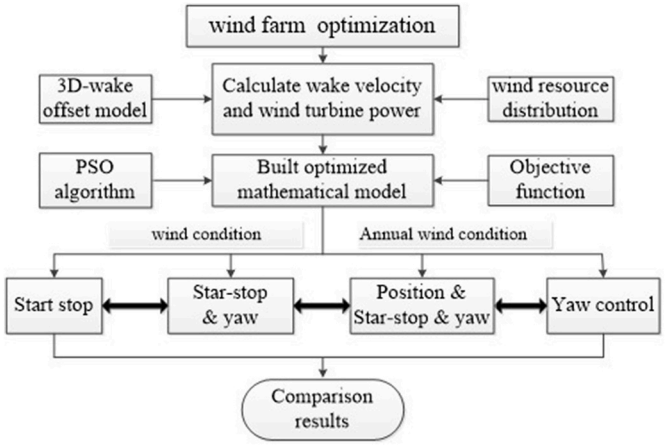

Fig. 1. flow chart of overall methodology.

2. Wind turbines offset wake model

2.1. Improved 3D wake model

In this paper, it was assumed that there was no wake generated from stopped wind turbines, as validated by previous research [27]. When the downstream wind turbine is outside the wake edge of the upstream wind turbine, its incoming wind speed remains unaffected by the upstream wind turbine. According to the observations made by Howland [11], the wake center of a wind turbine experiences an offset when it is in the yaw state. Dou [28] quantified this offset distance as *Yoffset* from the center of the wake region. The offset distance can be mathematically expressed as follows:

$$\frac{Yoffset}{D} = \delta(CT\sin\gamma)^{\zeta}\cos^{2\zeta}\gamma\sqrt{\frac{x}{D}} + \frac{drt}{D}\sin\gamma \tag{1}$$

Where CT is the thrust coefficient of a wind turbine; γ is the wind turbine yaw angle; D is the wind turbine rotor radius; X is the distance downstream of the wind turbine wake region; *drt* is the distance from the rotor center to the tower center; ζ is a fitting parameter of 0.75; δ is a function of CT: $\delta = 0.603CT$.

Dou [28] introduced a wake model for a yawing wind turbine and validated its accuracy through wind tunnel experiments. The velocity distribution within the wake region can be mathematically expressed as follows:

$$\frac{U}{Uh} = 1 - \left(1 - \sqrt{1 - \frac{CT\cos\gamma}{8\sigma^2 yaw}}\right) \times \exp\left[-\frac{1}{2\sigma^2 yaw}\left(\frac{y - y_*}{D\cos\gamma}\right)^2\right] \tag{2}$$

$$\sigma yaw = k\Big/x(D\cos\gamma) + \sqrt{\beta}\Big/5 \tag{3}$$

$$\beta = \left(1 + \sqrt{1 - CT\cos\gamma}\Big/2\sqrt{1 - CT\cos\gamma}\right) \tag{4}$$

Where y is the distance between wake center and required point; y* is offset distance; k is a parameter that can be determined based on the local meteorological conditions of the wind farm [29]. The velocity distribution within the wake region downstream of the wind turbine is shown in Fig. 2. Where, ΔU represents the velocity deficit in the wake; Y_{offset} is the distance between the wake center and Y/D = 0 line, and R_{dl} and R_{dr} represent the distance between the wake edges and wake center. In Fig. 2, we estimate the distances from the wake edges to the line

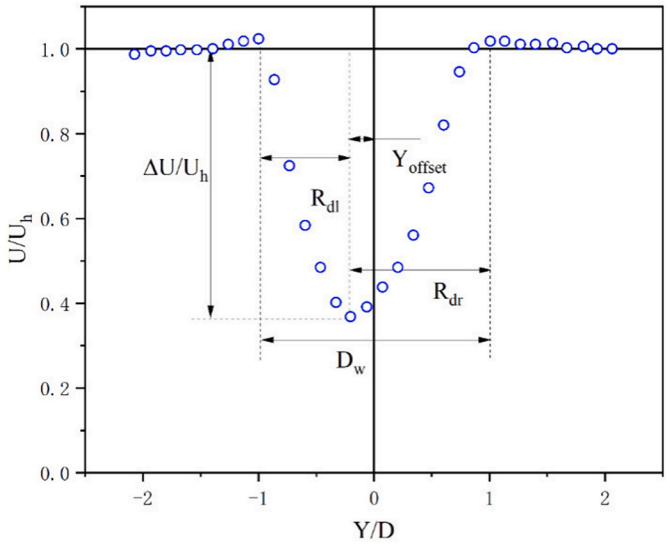

Fig. 2. Wind turbine wake area speed distribution in yawing condition.

where Y/D = 0, which leads to the ratio of R_{dr} to R_{dl}. As the wake model doesn't depend on the precise values of R_{dr}/R_{dl}, the data in Fig. 2 has been roughly smoothed for values under the same yaw angle conditions. This smoothing was done to more clearly illustrate the asymmetrical characteristic.

The downstream wind turbines of a wind farm are expected to be affected by the wake of multiple upstream wind turbines. Katic [30] assumes a linear superposition of the velocity deficit squared. This can be expressed as

$$(Uh - Ui)^2 = \sum_j (Uh - Uj, i)^2 \tag{5}$$

Where Ui, j is the wind speed of upstream wind turbine j at the position i; Ui is the wind speed of wind turbine at position i.

$$P = \frac{1}{2}\rho A U^3 Cp(a, \gamma) \tag{6}$$

equation (6) is a wind turbine power function. where ρ is the air density; A is the swept area of the wind turbine blades; U is the average wind speed induced by a wind turbine; Cp is the power coefficient which is the function of angle of attack α and yaw angle γ; it can be written as $Cp = 4a(\cos(\beta\gamma) - a)^2$; β is a constant [31], which equals to 0.785.

3. CR wind farm wind resource distribution

To investigate the impact of wind turbine active controlled operation on the annual power output of a wind farm, it is essential to obtain local wind resource data for the specific wind farm site. In the case of the Chapman Ranch (CR) wind farm, historical wind resource data from 1999 to 2009 was utilized [32]. This data was obtained from the National Oceanic and Atmospheric Administration's National Centers for Environmental Prediction (NCEP).

The dataset provides wind resource information with a spatial resolution of 1/3° × 1/3°. The wind speed interval in the dataset is 1 h, allowing for a detailed analysis of wind conditions over time. By specifying the latitude and longitude of the desired location measurement points within the wind farm, wind resource data can be extracted from the dataset. This process results in a total of 96,432 data points spanning a period of 10 years.

Fig. 3 shows the probability distribution of wind speed in the CR wind farm. The wind speed range is divided into 36 sections with intervals of 0.5 m/s. The occurrence probability of each wind speed interval is calculated based on 10 years of data. From the figure, it can be observed that the highest occurrence probability of wind speeds in the CR wind farm is concentrated between 2.5 m/s and 6.0 m/s. The probability of occurrence within this range is approximately 45 %. This indicates that wind speeds within this range are most frequently observed in the CR wind farm.

It's worth noting that the wind speed data provided by the NCEP were measured at a height of 10m. To calculate the wind turbine power, these measurements need to be converted to wind speeds at the hub height of the wind turbine. This conversion is necessary to ensure accurate estimation of the wind turbine's performance based on the provided wind speed data. The conversion of wind speed at measurement location to the wind speed at the hub height of a wind turbine can be achieved using equation (7).

$$\frac{Uh}{U1} = \left(\frac{Zh}{Z1}\right)^p \tag{7}$$

where $U1$ is the wind speed at measurement location; Uh is the wind speed at the hub height of a wind turbine; $Z1$ is the height at measurement location; Zh is the hub height of a wind turbine; p is a parameter that takes a value of 0.14 for the CR wind farm [24].

Fig. 4 represents the probability distribution of wind direction in the CR wind farm. The wind direction range is divided into 36 sections with intervals of 10°. By analyzing 10 years of data, the probability of occurrence for each wind direction interval is calculated. Based on

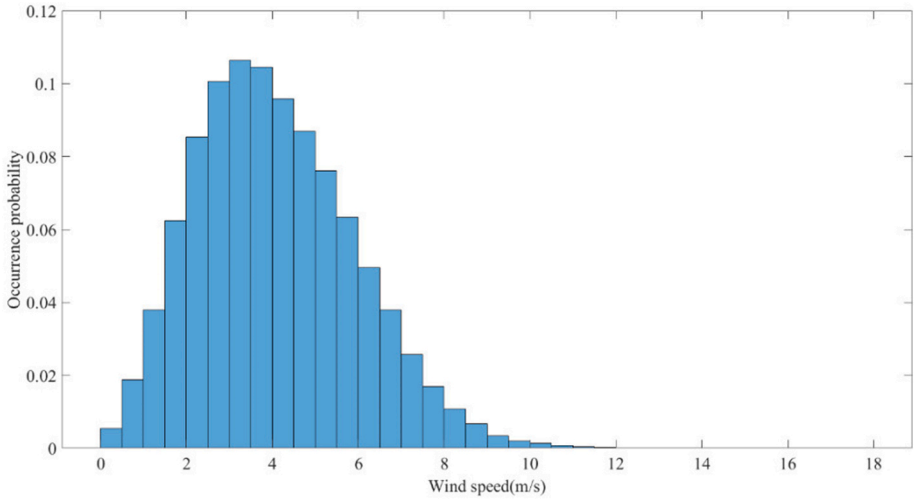

Fig. 3. Probability distribution of wind speed.

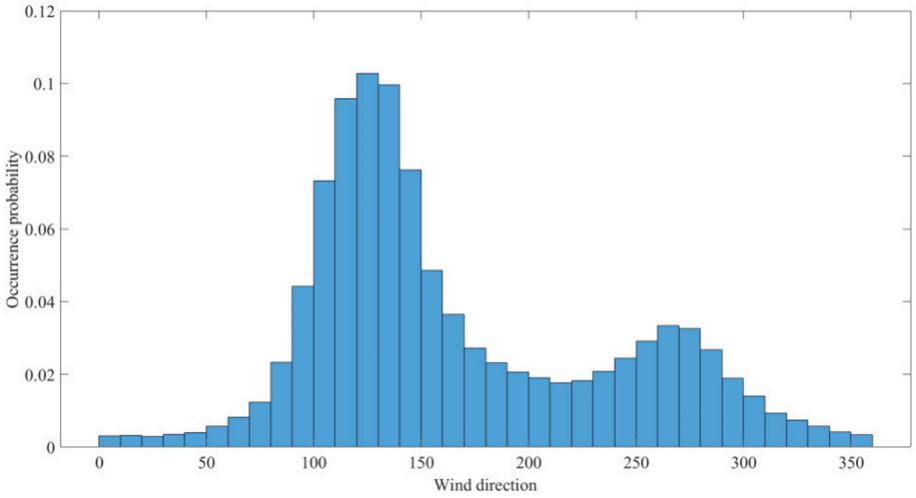

Fig. 4. Probability distribution of wind direction.

Fig. 3, it can be observed that the highest probability of wind direction occurrence in the CR wind farm is concentrated in two main ranges: from 100° to 150° and from 250° to 300°. These two ranges collectively account for approximately 60 % of the probability of wind direction occurrence.

Fig. 5 illustrates the wind condition probability distribution, which is derived by combining the probability distributions of wind speed and wind direction in the CR wind farm. A total of 1296 wind condition possibilities were identified with intervals of 0.5 m/s for wind speed and 10° for wind direction. By analyzing the probabilities of occurrence for each wind condition, Fig. 4 provides insights into the likelihood of different wind conditions in the CR wind farm. It indicates that the highest probability of wind conditions occurring, reaching 31.1 %, is observed when the wind speed ranges from 2.5 m/s to 6.0 m/s and the wind direction ranges from 100° to 145°.

This probability distribution of wind conditions serves as a valuable dataset for assessing the annual power output of the wind farm, as it provides an understanding of the likelihood of different wind speed and wind direction combinations. This information can be utilized in the subsequent sections of the study to evaluate and optimize the performance of the wind farm.

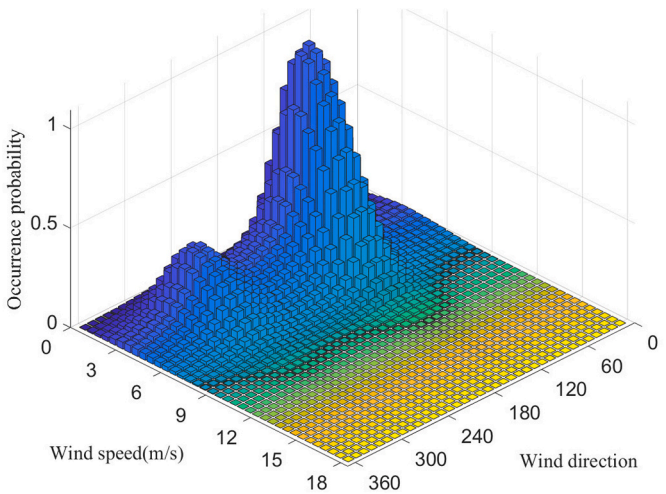

Fig. 5. Probability distribution of wind conditions.

4. Start/stop and yaw synchronous optimized strategy

4.1. Optimization of mathematical models

4.1.1. Objective function

To maximize the power output of a wind farm, the objective function can be defined using equation (8). The objective function aims to maximize the total power output of the wind farm by summing up the power generated by each individual wind turbine within the farm. The goal is to optimize the wind farm layout, start/stop strategy, and yaw control in order to achieve the highest possible power output.

$$maximize \quad Pwf = \sum_{i}^{n} Pwti(U, c, \gamma) \tag{8}$$

Where *Pwt* is the power output of a wind turbine; *U* is the average wind speed induced by the wind turbine; *c* is the start/stop controlled variable of the wind turbine; and γ is the yaw angle of the wind turbine. The average wind speed *U* of the downstream wind turbine is influenced by the upstream wind turbine through controlling its start-stop variable *c* and yaw angle γ.

4.1.2. Design variables and constraints

To determine the start-stop state of wind turbines in a wind farm, the start-stop variables of individual turbines can be set using a random number *r*1 in the range [0, 1], as shown in equation (9). The random number *r*1 is rounded to either 0 or 1, where 0 indicates a wind turbine in a stopped state and 1 represents a wind turbine in normal operation. By rounding the random number *r*1 to the nearest integer, the start-stop factor of a wind turbine can only have two possibilities: 0 or 1.

$$c = \begin{cases} round(r1) = 0 \quad Stop\ operation \\ round(r1) = 1 \quad Normal\ operation \end{cases} \quad 0 \le r1 \le 1 \tag{9}$$

In addition to the start-stop design variables, the yaw angle γ of wind turbines can be considered as design variables:

$$\gamma = -30 + 60 r_2 \quad 0 \le r_2 \le 1 \tag{10}$$

Where r_2 is a random number in the range of [0, 1]. Then, the range of yaw angle is from −30° to 30°.

There will be some colliding wakes between wind turbines in CR wind farms if we do not consider the location of turbines as variables. The colliding wakes would multiply the turbulence intensity and not only increases the fatigue loads on the turbines, but might also impact the extreme loads. Therefore, in order to avoid colliding wakes and

reduce the influence of wake superposition on downstream wind turbines, the turbines positions in CR wind farms should be also considered as variables.

Therefore, three kinds of parameters are set as variables. They are start-stop, yaw angles and turbines positions.

4.1.3. Optimization algorithm and process

In this paper, the wind farm layout optimization involves solving a multi-dimensional problem with multiple variables. To find the best combination of these variables, a global search approach is necessary. Numerous intelligent algorithms, such as Genetic Algorithms (GA), Particle Swarm Optimization (PSO), and others, exist to tackle wind farm layout optimization problems. In this study, we've chosen to employ PSO as our optimization method. The choice of PSO was based on its notable advantages including its optimization efficiency, simplicity of implementation, and limited algorithmic parameters. While GA could also serve this purpose, the focal point of our paper is not a comparative analysis of different intelligent algorithms. Instead, our primary focus is on proposing a synchronized optimization model that integrates both start-stop and yaw control for wind turbines in a wind farm.

In this specific implementation, the dimension of the particles is set to 2n, where n represents the number of wind turbines in the wind farm. The first n dimensions correspond to the start-stop variables of the wind turbines, while the next n dimensions represent the yaw angles of the wind turbines. To ensure the particles' values remain within reasonable bounds, the boundaries of the particles are set between [0, 1]. This constraint ensures that the start-stop variables and yaw angles fall within feasible ranges. Furthermore, the number of populations in the PSO algorithm is set to 10n, which determines the size of the swarm and the number of iterations in the optimization process. The larger the population size, the more extensive the search space exploration, potentially leading to better optimization results.

Fig. 6 shows the flowchart of wind turbine start-stop, yaw angle and turbines positions optimization using PSO. The specific process is : ① Set the wind turbine parameters and import the wind resource data. ② Initialize the population with each element being a random number between [0, 1]. ③ Translate the solution into start-stop, yaw angle controlling and turbines positions. ④ sort wind turbines of the wind farm based on the wind direction. ⑤ Determine the wake shading of each wind turbine by the upstream wind turbines.⑥ Calculate the inflow wind speed of each wind turbine based on the ranking of wind turbines. For wind turbines affected by an upstream wind turbine, use the 3D wake model to calculate the inflow wind speed. For wind turbines affected by multiple upstream wind turbines, use the 3D wake superposition model to calculate the inflow wind speed. ⑦ Calculate the fitness of each individual and update the best position of the population. ⑧ Determine if the algorithm has converged. If not, return to process ③ and iterate until reaching the maximum iterations. Then, output the optimal results.

4.2. Optimized results under a certain wind condition

In order to investigate the overall power output improvement of the actual wind farm through start-stop and yaw controlling optimization, the CR wind farm is chosen as the baseline wind farm. It has 81 Nordex

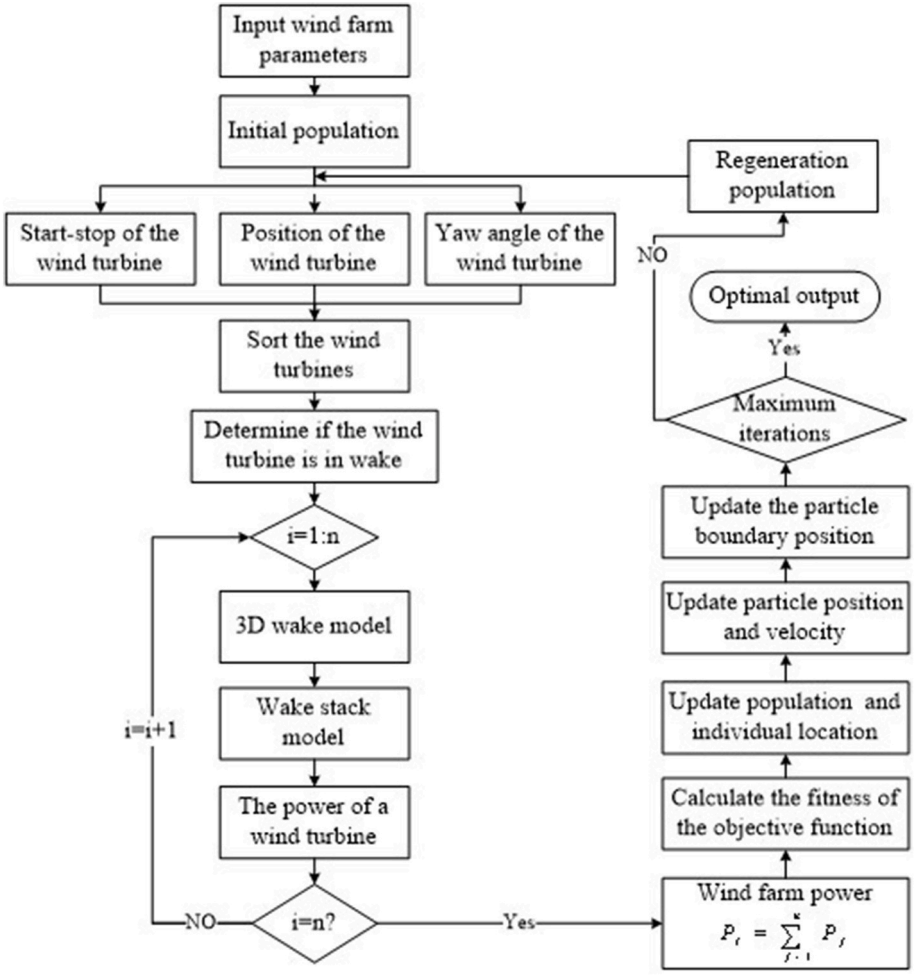

Fig. 6. Flow chart of wind turbine start/stop and yaw angle controlling optimization.

AW125/3000 wind turbines with a rotor diameter of 125m and a hub height of 87.5m. Fig. 7 illustrates the micro layout of the CR wind farm, where the black arrow represents an inflow angle of 180°. Under a specific wind condition, the parameters are as follows: the inflow wind speed is 5.5 m/s, the turbulence intensity (TI) is 10 %, and the wind turbine thrust coefficient (CT) is 0.86. F.Gonzalez-Longatt [33] has indicated that the wake coefficients were different when exposed to the variable wind speed of one year. Our choice of 5.5 m/s as the representative wind speed is based on the predominant wind speed distribution in the CR wind farm, which primarily falls between 2.5 m/s and 6 m/s, as depicted in Figs. 3 and 5.

Fig. 8 illustrates the iteration process of the start-stop, yaw angle controlling and wind turbines positions simultaneously optimization for the CR wind farm. The convergence times are increased as the design variables increase. Notably, the overall power output for the start-stop, yaw and turbines positions synchronous optimization is higher compared to the other three cases.

Fig. 9 shows the optimized results of the wind farm layout for the four cases: yaw angle control, start-stop optimization, start-stop & yaw angle control and Synchronous optimization of start-stop & yaw & turbines positions. The relevant symbols in Fig. 9 are explained as follows: the rectangle represents a single wind turbine; the black arrow indicates the inflow wind direction of 180°; the non-yawed wind turbine is displayed with the long side of the rectangle perpendicular to the X-axis. If the yaw angle is positive for clockwise rotation, the values of the yaw angle are displayed in the upper left corner of each rectangle. Light colors in the rectangles represent higher power output of the wind turbines, while dark colors indicate relatively lower power output. The red boxes in Fig. 9(b)–(c) and (d) represent the stopped wind turbines. In Fig. 9(b), all wind turbines in the wind farm have a yaw angle of 0° because only the start-stop parameters are optimized variables.

In Fig. 9(b), nine wind turbines are shut down as part of the start-stop optimization. In Fig. 9(c), five wind turbines are stopped in the start-stop and yaw angle synchronous optimization, all of which are in a lower power output condition. The power output efficiency of the downstream wind turbines has been improved by stopping these five wind turbines. However, we notice that the distance between turbines is too close (smaller than 5D) to reduce the wake effects in the red round areas from Fig. 9(a)–9(c). The colliding wakes could multiply the turbulence intensity. This escalation can not only heighten the fatigue loads on the turbines but might also influence the extreme loads. To reduce these adverse effects, the turbines positions must be adjusted. Fig. 9(d) shows the synchronously optimized results considering turbines positions, start-stop and yaw control. The distance between upstream and downstream turbine is greater than 5D, which can alleviate or even eliminate

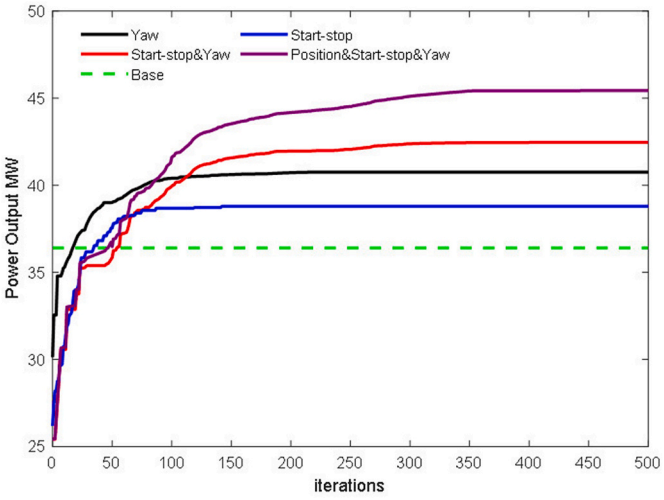

Fig. 8. Iteration of start/stop, yaw controlling and turbines positions of wind farm.

colliding wake combined start-stop and yaw angle controlling optimization.

Table 1 presents the overall power output of the CR wind farm under different optimized modes. Based on the findings from Figs. 8 and 9, and Table 1, the following comparisons can be made: if the wind turbines positions are not changed, there will be an increase of the power output for the three cases (yaw, start–stop and start-stop with yaw). For example, the power output for the case of start-stop and yaw optimization is 42.86 MW, representing an increase of 17.7 % compared to the normal operation. But there could be an influence of wake superposition on downstream wind turbines. By considering start-stop, yaw angle and turbines positions simultaneous optimization in the CR wind farm, the power output reaches 45.88 MW, demonstrating a significant increase of 26.01 % compared to the normal operation. These results indicate that the combined optimization of start-stop, yaw control and turbines positions not only yields the highest improvement in the overall power output, but also can reduce the impact of wake superposition on the downstream wind turbines.

4.3. *Optimized results of annual wind condition*

According to the results of the four cases in Section 4.2, it is clear that the synchronous optimization of case 4 has the most significant improvement in the power output of the CR wind farm, followed by the

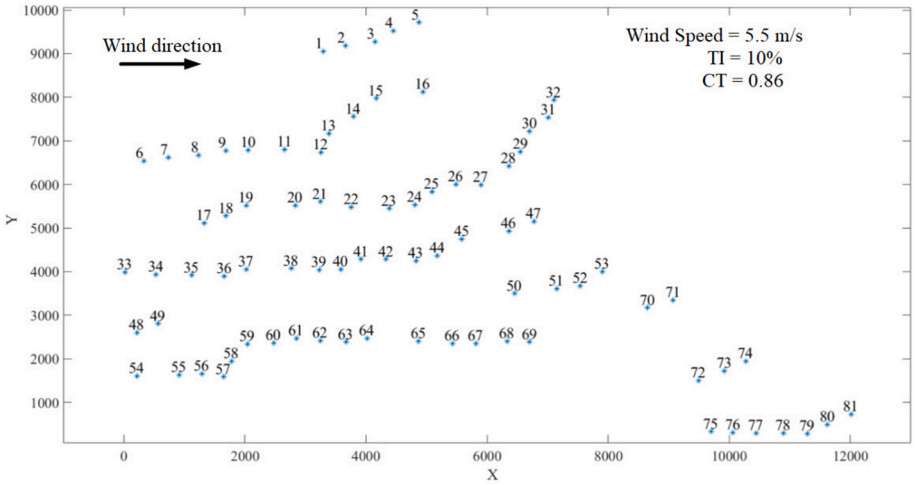

Fig. 7. CR wind farm layout.

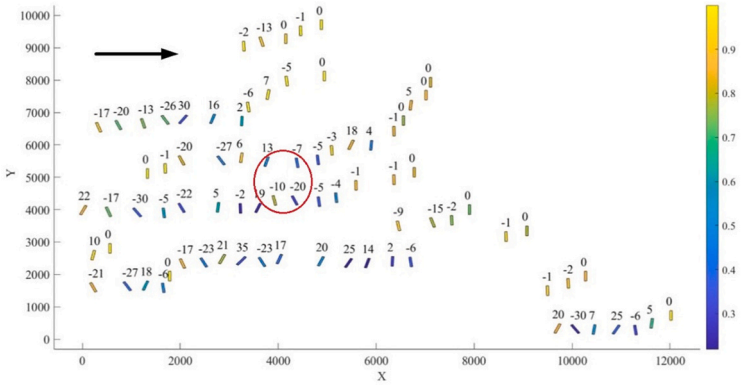

(a)

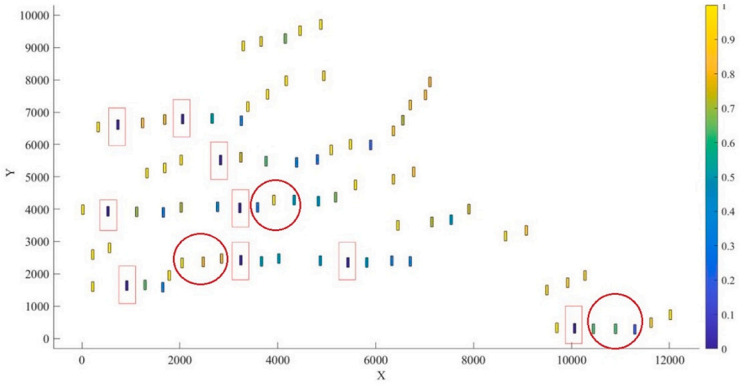

(b)

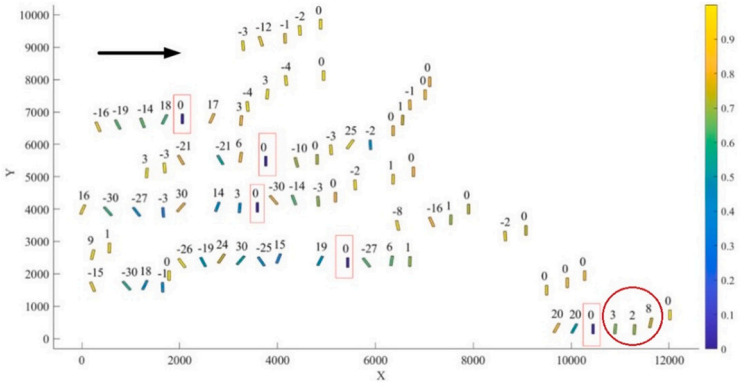

(c)

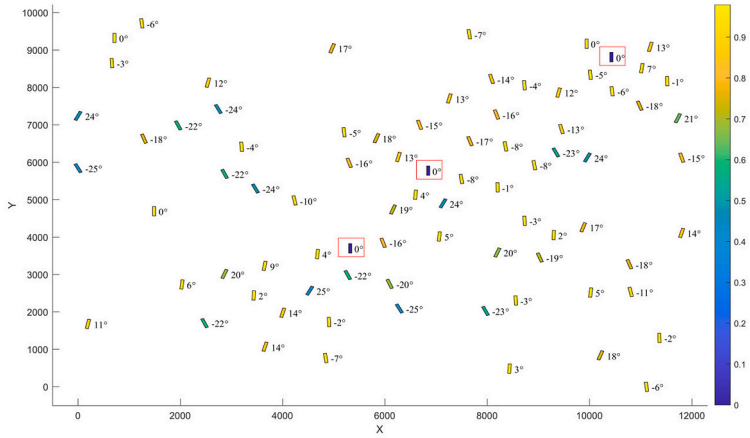

(d)

Fig. 9. the wind farm layout optimization for four cases.

Table 1
Wind farm power output under different optimization modes.

Optimization method	Power output	Optimized increased	Number of wind turbines stopped
Normal operation	36.41 MW	0	0
Yaw optimization	40.75 MW	11.9 %	0
Start-stop optimization	38.78 MW	6.53 %	9
Start-stop and yaw optimization	42.86 MW	17.7 %	5
Start-stop, yaw and turbines positions optimization	45.88 MW	26.01 %	3

optimization of the start-stop and yaw angle control. Similarly, when comparing the overall power performance of annual wind conditions for CR wind farms, these four cases are selected as the research subjects. Firstly, the power output of the wind farm under different wind conditions can be calculated. Then, the annual power output of the wind farm is obtained using the following formula:

$$Ptotal = \sum_{i}^{Np} Pi \cdot Pwfi \cdot 365 \cdot 24 \tag{11}$$

Where *Np* is the number of wind conditions; *Pi* is the probability of the *i*-th wind condition; *Pwfi* is the power output of the wind farm under the *i*-th wind condition.

It should be note that a total of 1296 different wind conditions according to section 3 are considered to optimize the CR wind farm layout. That means we have considered a wider wind speed and different wind direction when we optimize the CR wind farm layout for the annual power output.

The power output improvement rates for different wind speed and wind direction are shown in Fig. 10. It can be observed that start-stop, yaw control and turbines positions simultaneous optimization leads to the largest improvement in power output for different wind conditions, followed by start-stop and yaw control. Notify, when the wind speed reaches 8 m/s or higher, the optimization results of four cases cannot significantly enhance the power output of the wind farm. This can be attributed to the wind speed nearing the rated power wind speed of the wind turbines, where the power loss incurred by shutting down the wind turbines outweighs the power increase achieved by reducing the wake effect.

Fig. 11 is the power output corresponding to each wind condition. It indicates that in the case of low wind speed, the overall power output for case 4 (start-stop, yaw control and turbines positions optimization) surpasses the other three cases. However, when the inflow wind speed of the wind farm exceeds 10 m/s, the improvement in annual power output for all cases becomes relatively small.

Table 2 presents the annual power output of the CR wind farm under different optimization scenarios. Because of considering the different wind conditions, the increment of the annual power output is not significant for the four cases. However, when considering synchronized start-stop, yaw and turbines positions optimization, the annual power output reaches 453,007 MW-h, still exhibiting an increase of 8.85 %. These results clearly demonstrate that the maximum annual power output of the CR wind farm is achieved when the parameters of start-stop, yaw control and turbines positions are considered.

5. Conclusion

In this paper, the focus is on improving the power output of an existing wind farm considering the change of start-stop, yaw control and turbines positions. To achieve this, a modified 3D-biased wake model is employed to calculate the wake speed of each wind turbine in the wind farm. Additionally, a random number distribution within the range of [0, 1] is utilized to control the start-stop state of the wind turbines. In order to study the results of the wind farm layout considering different design variables, four cases (case 1: yaw control; case 2: start-stop; case 3: start-stop & yaw control; case 4: start-stop, yaw control and turbines positions) are formulated. Then, a mathematical model is formulated with the objective of maximizing the overall power output. Through the use of the PSO algorithm, some important conclusions have been drawn based on the CR wind farm and wind resource data.

(1) When analyzing the power output of the CR wind farm under single wind conditions, it is evident that optimization techniques have led to significant improvements. Comparing the results to the original wind farm power output, the optimization of the previous three cases (yaw control, start-stop and start-stop & yaw control) can improve the power output, but can lead to colliding wake in some fields of the CR wind farm. It may produce high turbulence intensity and raise fatigue load. Therefore, the

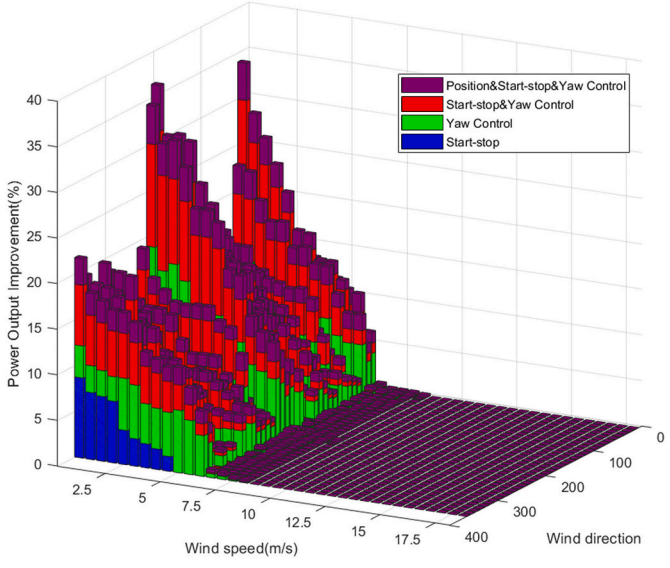

Fig. 10. Annual power improvement rate of the wind farm for three optimized models.

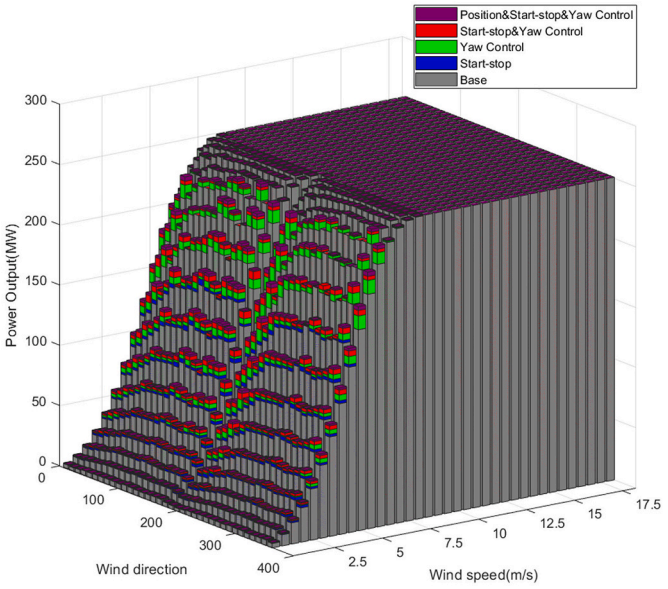

Fig. 11. Power corresponding to each wind condition.

Table 2
Comparison of wind farm power output.

	annual power output (MW·h)	imropvement rate (%)
Base power	416176	0
Start/stop	422876	1.61
Yaw angle	443723	6.62
Start-stop and yaw angle	449387	7.68
Start-stop, yaw angle and position	453007	8.85

turbines positions should be changed to avoid the colliding wake. The optimized result of considering start-stop, yaw and turbines positions has yielded the highest overall power output of 45.88 MW, showing a remarkable 26.0 % increase. These findings highlight the effectiveness of synchronous optimization in maximizing the wind farm's overall power output.

(2) Using the wind resource data of the CR wind farm from 2000 to 2009, the annual power output of the wind farm is calculated after optimization. Comparing it to the base wind farm, the annual power output is found to increase by 1.61 % when considering wind turbine start-stop optimization. Furthermore, with the implementation of yaw angle control, the annual power output can be increased by 6.62 %. The annual power output can be increased by 7.68 % because of considering start-stop and yaw angle control. However, the most significant improvement is achieved when start-stop, yaw control and turbines positions are synchronized, resulting in a 8.85 % increase in the annual power output. Additionally, it is observed that the synchronization of start-stop yaw control and turbines positions optimization has the greatest impact on the overall power output of the wind farm when the wind speed is low (below 8 m/s). Conversely, as the wind speed increases (above 8 m/s), the effect on the overall power output becomes less pronounced.

There are still two points should be improved. Different optimized algorithm could get different results. It's of interesting for us to study wind farm layout using some new intelligent algorithms. Another issue is that the effect of wake on mechanical loads and fatigue loads should be considered when optimizing wind farm layout.

Funding statement

This work was supported by the National Natural Science Foundation of China (No.51975190) and the Green Industry Science and Technology Leading Plan of Hubei University of Technology for Excellent Young Scholars (No.XJ2021001201).

CRediT authorship contribution statement

Quan Wang: Writing – original draft, Writing – review & editing. **Tangjie Xu:** Data curation, Validation. **Dominic von Terzi:** Visualization. **Wei Xia:** Conceptualization. **Zhenhai Wang:** Investigation. **Haoran Zhang:** Resources.

Declaration of competing interest

The authors declare that they have no known competing financial interests or personal relationships that could have appeared to influence the work reported in this paper.

References

[1] N.O. Jensen, A Note on Wind Generator Interaction, Citeseer, 1983.
[2] I. Katic, J. HøJSTRUP, N.O. Jensen, A simple model for cluster efficiency, in: Proceedings of the European Wind Energy Association Conference and Exhibition, F, A. Raguzzi Rome, Italy, 1986.
[3] S. Frandsen, R. Barthelmie, S. Pryor, et al., Analytical modelling of wind speed deficit in large offshore wind farms, Wind Energy: Int. J. Prog. Appl. Wind Power Convers.Technol. 9 (1-2) (2006) 39–53.
[4] M. Abkar, F. Porté-Agel, Influence of atmospheric stability on wind-turbine wakes: a large-eddy simulation study, Phys. Fluid. 27 (3) (2015) 035104.
[5] Y.-T. Wu, F. Porté-Agel, Large-eddy simulation of wind-turbine wakes: evaluation of turbine parametrisations, Boundary-Layer Meteorol. 138 (3) (2011) 345–366.
[6] T. Ishihara, G.-W. Qian, A new Gaussian-based analytical wake model for wind turbines considering ambient turbulence intensities and thrust coefficient effects, J. Wind Eng. Ind. Aerod. 177 (2018) 275–292.
[7] Majid Bastankhah, Fernando Porté-Agel, A new analytical model for wind-turbine wakes, Renew. Energy 70 (2014) 116–123.
[8] Siyu Tao, Qingshan Xu, et al., Wind farm layout optimization with a three-dimensional Gaussian wake model, Renew. Energy 159 (2020) 553–569.
[9] Guo-Wei Qian, Takeshi Ishihara, Wind farm power maximization through wake steering with a new multiple wake model for prediction of turbulence intensity, Energy 220 (2021) 119680.
[10] Rezvane S. Mirsane, Farschad Torabi, An innovative method of investigating the wind turbine's inflow speed in a wind farmdue to the multiple wake effect issue, Energy Convers. Manag. 269 (2022) 116077.
[11] M.F. Howland, J. Bossuyt, L.A. MartíNEZ-Tossas, et al., Wake structure in actuator disk models of wind turbines in yaw under uniform inflow conditions, J. Renew. Sustain. Energy 8 (4) (2016) 043301.
[12] P. Fleming, J. Annoni, J.J. Shah, et al., Field test of wake steering at an offshore wind farm, Wind Energy Sci. 2 (1) (2017) 229–239.
[13] P.M. Gebraad, F.W. Teeuwisse, J. Van Wingerden, et al., Wind plant power optimization through yaw control using a parametric model for wake effects—a CFD simulation study, Wind Energy 19 (1) (2016) 95–114.
[14] H. Ma, M. Ge, G. Wu, et al., Formulas of the optimized yaw angles for cooperative control of wind farms with aligned turbines to maximize the power production, Appl. Energy 303 (2021) 117691.
[15] J. Park, K.H. Law, A data-driven, cooperative wind farm control to maximize the total power production, Appl. Energy 165 (2016) 151–165.
[16] B. Dou, T. Qu, L. Lei, et al., Optimization of wind turbine yaw angles in a wind farm using a three-dimensional yawed wake model, Energy 209 (2020) 118415.
[17] F. Haces-Fernandez, H. Li, D. Ramirez, Improving wind farm power output through deactivating selected wind turbines, Energy Convers. Manag. 187 (2019) 407–422.
[18] Zhenyu Lei, Shangce Gao, et al., An adaptive replacement strategy-incorporated particle swarm optimizer for wind farm layout optimization, Energy Convers. Manag. 269 (2022) 116174.
[19] Qingshan Yang, Hang Li, Li Tian, Xuhong Zhou, Wind farm layout optimization for levelized cost of energy minimization with combined analytical wake model and hybrid optimization strategy, Energy Convers. Manag. 248 (2021) 114778.
[20] Shriya V. Nagpal, M. Vivienne Liu, C. Lindsay Anderson, A comparison of deterministic refinement techniques for wind farm layout optimization, Renew. Energy 168 (2021) 581–592.
[21] Lichao Cao, Mingwei Ge, et al., Wind farm layout optimization to minimize the wake induced turbulence effect on wind turbines, Appl. Energy 323 (2022) 119599.
[22] Yi Wen, Mengxuan Song, Jun Wang, Wind farm layout optimization with uncertain wind condition, Energy Convers. Manag. 256 (2022) 115347.
[23] Kaixuan Chen, Lin Jin, et al., Joint optimization of wind farm layout considering optimal control, Renew. Energy 182 (2022) 787–796.
[24] Nicol_o Pollini, Topology optimization of wind farm layouts, Renew. Energy 195 (2022) 1015–1927.
[25] R. Sohail, Reddy. Wind Farm Layout Optimization (WindFLO) : an advanced framework for fast wind farm analysis and optimization, Appl. Energy (2020) 115090.
[26] Haiying Sun, Hongxing Yang, Wind farm layout and hub height optimization with a novel wake model, Appl. Energy (2023) 121554.
[27] C.L. Archer, A. Vasel-Be-Hagh, et al., Review and evaluation of wake loss models for wind energy applications, Appl. Energy 226 (2018) 1187–1207.
[28] B. Dou, M. Guala, L. Lei, et al., Wake model for horizontal-axis wind and hydrokinetic turbines in yawed conditions, Appl. Energy 242 (2019) 1383–1395.
[29] M. Bastankhah, F. Porté-Agel, A new analytical model for wind-turbine wakes, Renew. Energy 70 (2014) 116–123.
[30] I. Katic, J. HøJSTRUP, N.O. Jensen, A simple model for cluster efficiency, in: Proceedings of the European Wind Energy Association Conference and Exhibition, F, A. Raguzzi Rome, Italy, 1986.
[31] J. Park, K.H. Law, Cooperative wind turbine control for maximizing wind farm power using sequential convex programming, Energy Convers. Manag. 101 (2015) 295–316.
[32] S. Saha, Documentation of the Hourly Time Series from the NCEP Climate Forecast System Reanalysis (1979-2009), EMC/NCEP/NOAA, 2009.
[33] F. González-Longatt, P. Wall, V. Terzija, Wake effect in wind farm performance: Steady-state and dynamic behavior, Renew. Energy 39 (2012) 329–338.